Precocious cerebellum development and improved motor functions in mice lacking the astrocyte cilium-, patched 1-associated Gpr37l1 receptor

Daniela Marazziti[1], Chiara Di Pietro[1], Elisabetta Golini, Silvia Mandillo, Gina La Sala, Rafaele Matteoni, and Glauco P. Tocchini-Valentini[2]

Consiglio Nazionale delle Ricerche, European Mouse Mutant Archive-Infrafrontier-International Mouse Phenotyping Consortium, Istituto di Biologia Cellulare e Neurobiologia, I-00015 Monterotondo Scalo (Rome), Italy

In the developing cerebellum, the proliferation and differentiation of glial and neuronal cell types depend on the modulation of the sonic hedgehog (Shh) signaling pathway. The vertebrate G-protein-coupled receptor 37-like 1 (*GPR37L1*) gene encodes a putative G-protein–coupled receptor that is expressed in newborn and adult cerebellar Bergmann glia astrocytes. This study shows that the ablation of the murine *Gpr37l1* gene results in premature down-regulation of proliferation of granule neuron precursors and precocious maturation of Bergmann glia and Purkinje neurons. These alterations are accompanied by improved adult motor learning and coordination. *Gpr37l1*$^{-/-}$ mice also exhibit specific modifications of the Shh signaling cascade. Specific assays show that in Bergmann glia cells Gpr37l1 is associated with primary cilium membranes and it specifically interacts and colocalizes with the Shh primary receptor, patched 1. These findings indicate that the patched 1–associated Gpr37l1 receptor participates in the regulation of postnatal cerebellum development by modulating the Shh pathway.

mutant mouse model | mitogenic signaling

The cytoarchitecture of the cerebellum includes only a few cell types, thus offering a convenient system to study the regulatory pathways that coordinate brain cell proliferation, survival, and differentiation (1). Granule and Purkinje cell neurons and Bergmann glia astrocytes concomitantly differentiate in the developing mouse cerebellum. In the earliest postnatal period, the external granular layer (EGL) contains granule cell precursors (GCPs). Their proliferation is sustained by interneuronal contacts, whereas interactions with astrocytes inhibit the mitotic cycle and induce their differentiation (2). Postmitotic granule cells migrate along glial radial fibers, through the molecular layer (ML) and Purkinje cell layer (PCL), thus forming the internal granular layer (IGL) (3). Before the migratory process, in the inner EGL, each granule neuron generates a single axonal outgrowth, which extends during neuron migration along the glial processes, while producing bifurcate axonal fibers. These run parallel to the cerebellar pial surface and make synaptic contacts with the developing Purkinje cell arbors (3). At about 2 wk after birth, the EGL structure is not distinguishable anymore, and postmitotic granule cells have all completed their migration into the IGL (4).

The molecular regulation of this complex set of cellular interactions and differentiation events is only partially understood (5). The duration and intensity of the GCP proliferation phase determine the size of the mature granule cell pool and therefore influence the final morphology and physiology of the cerebellum (6). In the earliest postnatal stage, Purkinje neurons secrete the cholesterol-modified sonic hedgehog protein (Shh), which crucially stimulates postnatal GCP proliferation (7–9). Shh also affects the Bergmann glia population, promoting its maturation/differentiation (7). During postnatal cerebellar development, both glial astrocytes and GCPs express high levels of the Shh pathway components, including the transmembrane transporter-like patched 1 (Ptch1) and the seven-transmembrane span smoothened (Smo) proteins (10, 11). Shh signaling is regulated by several ligand-binding factors, including Ptch1, its primary receptor, and associated coreceptors (12, 13). The binding of Shh to the Ptch1 complex leads to the derepression of Smo. This in turn triggers an intracellular signal transduction cascade, with transactivation of several target genes (14). Many different proteins are involved in the regulation of the Shh mitogenic signal, but their specific roles and mechanisms of action are only partially established (10).

Mammalian genome-wide expression studies have identified gene sets whose transcripts and protein products are enriched in developing and adult cerebellar neurons and glial cells (15, 16). Among them, the *GPR37L1* gene was found highly expressed in developing (Cerebellar Development Transcriptome Database, accession no. CD06446) and adult Bergmann glia astrocytes (17). It was also identified as a modulator of the genesis and assembly of the primary cilium, a cellular organelle required for Shh–Smo signaling (18, 19). The vertebrate G-protein–coupled receptor 37 and G-protein–coupled receptor 37-like 1 (*GPR37* and *GPR37L1*) genes encode seven-transmembrane span proteins with amino acid sequence homology to

Significance

A new mouse mutant strain carrying a genetic deletion of the G-protein–coupled receptor 37l1 (*Gpr37l1*) was established and characterized. Null mutant animals exhibit specific alterations of postnatal cerebellar development, with premature down-regulation of granule neuron proliferation, precocious Bergmann glia, and Purkinje neuron maturation and layer formation. The postnatal expression of several components of the sonic hedgehog protein mitogenic pathway is consistently changed in cerebellar samples from Gpr37l1 knock-out mice. These alterations are associated with precocious juvenile motor abilities and improved adult motor learning and coordination. The Gpr37l1 and patched 1 proteins are found to colocalize and interact in Bergmann glia cells during cerebellar development. The reported experimental data indicate that Gpr37l1 participates in the regulation of sonic hedgehog signaling during postnatal cerebellar development.

G-protein–coupled receptors for the endothelin and bombesin peptides (17, 20, 21). Recently, the secreted neuro- and glio-protective glycoprotein prosaposin and derived peptides have been shown in vitro to interact with and activate both putative receptors (22).

To test a functional role of Gpr37l1 in cerebellar Shh signaling, a unique mouse strain with a targeted deletion of the *Gpr37l1* gene was produced and characterized. Homozygous null mutant mice exhibited specific alterations of postnatal cerebellar development, with premature down-regulation of GCP proliferation, precocious Bergmann glia, and Purkinje neuron maturation and cerebellar layer formation. *Gpr37l1*$^{-/-}$ mice also showed consistent changes of the postnatal expression levels of Shh and various components of its signaling pathway. Specific assays indicated that in Bergmann glia cells, Gpr37l1 is associated with primary cilium structures and interacts and colocalizes with Ptch1, during postnatal cerebellar development. Furthermore, premature cerebellar differentiation in the mutant mice is accompanied by specific changes in motor function development, including precocious juvenile motor abilities and improved adult motor learning and coordination. Taken together, the reported data indicate that Gpr37l1 participates in the cerebellar development by modulating Shh signaling.

Results

Gpr37l1 Is Expressed by Bergmann Glia Cells.
Cerebellar glial cell bodies and fibers of wild-type pups and adult mice were immunolabeled with antibodies specific for Gpr37l1 (Fig. 1A), consistent with the expression pattern of the *Gpr37l1* gene by in situ hybridization (ISH) in whole brain sections of newborn and adult C57BL/6J mice (Fig. S1 A and B) (17). The receptor protein was found colocalized with the astrocytic glial high-affinity glutamate transporter (Glast), with typical staining of reticular and fibrous structures, in the ML and EGL, respectively (Fig. 1B; see Fig. 3A). It was also found associated with the basal membrane of Bergmann glia cell primary cilia, where it colocalizes with ADP ribosylation factor-like protein 13B (Arl13b), a small ciliary GTPase enzyme (Fig. 1C). Its expression, from postnatal day (P) 5 to the adult stage, was confirmed by immunoblotting of cerebellar extracts from wild-type males (Fig. S1 E and F). A unique mutant mouse strain (*Gpr37l1*$^{-/-}$) was established by targeted gene deletion (*SI Materials and Methods* and Fig. S1C). Both heterozygous and homozygous mutant animals generated fully vital and fertile offspring, without anatomical abnormalities (Fig.

S2) and no alteration of adult cerebellar layer cytoanatomy and organization (Fig. S2A; see Fig. S5 C and E).

Premature Down-Regulation of EGL Proliferation in Gpr37l1$^{-/-}$ Mice.
Cerebellar EGL neurons were stained with the Hoechst nuclear dye in midsagittal sections from wild-type or *Gpr37l1*$^{-/-}$ littermates at distinct postnatal stages. Both genotype groups showed similar folia anatomy at all stages studied (Fig. 1D and Fig. S2) but the average thickness of individual cerebellar layers was altered in P10 and, less markedly, in P15 null mutant animals [Fig. 1D and Fig. S2B). At P10, they exhibited a decrease in the EGL (t test, $t_{(1,4)} = 3.43$, $P < 0.05$], a marked increase in the ML [t test, $t_{(1,4)} = -4.14$, $P < 0.05$] and no variation in the IGL (Fig. 1E). No significant difference was detected in P0, P3, and P5 pups (Fig. S2).

EGL neuron proliferation was studied in P3, P5, and P7 cerebellar samples of wild-type or *Gpr37l1*$^{-/-}$ littermates upon in vivo 5-bromo-2′-deoxyuridine (BrdU) incorporation followed by immunostaining 2 h postinjection. The overall localization of BrdU incorporation was similar, but in the null mutant pups the average number of BrdU-positive cells was increased at P3 and reduced at P7, whereas it did not vary at P5, in comparison with wild-type littermates [Fig. 2 A and B; ANOVA: effect of age, $F_{(2,12)} = 8.46$, $P = 0.005$; effect of genotype, $F_{(1,12)} = 0.043$, not significant (NS); age × genotype, $F_{(2,12)} = 10.26$, $P = 0.0025$]. Similar results were obtained with the quantitative analysis of premitotic and mitotic EGL neurons, following immunolabeling of the phosphohistone 3 (PH3) protein complex, at P0, P3, P5, P10, and P15 postnatal stages. In comparison with wild-type littermates, *Gpr37l1*$^{-/-}$ pups exhibited a decrease in the total number of PH3-positive cells at P10 (Fig. 2C; t test, $t_{(1,6)} = 2.37$, $P = 0.05$). This was related to a decrease in the number of premitotic G2-phase cells at P10 [t test, $t_{(1,6)} = 2.70$, $P < 0.05$] and P15 [t test, $t_{(1,4)} = 3.25$, $P < 0.05$], whereas the count of mitotic M-phase cells was never altered (Fig. 2C).

Altered EGL Differentiation in Gpr37l1$^{-/-}$ Mice.
The outer and inner portions of the EGL (oEGL and iEGL) are distinguished on the basis of the relative prevalence of proliferating or differentiating granule neurons, which can be labeled with specific antibodies against proliferating cell nuclear antigen (Pcna) for oEGL, or axonal contactin 2 glycoprotein (Cntn2/Tag1) and the post-mitotic nuclear cyclin-dependent kinase inhibitor 1B (Cdkn1B/p27-Kip1) protein for iEGL (Fig. S3). Examination of cerebellar sections after Pcna and Tag1 double immunolabeling suggested
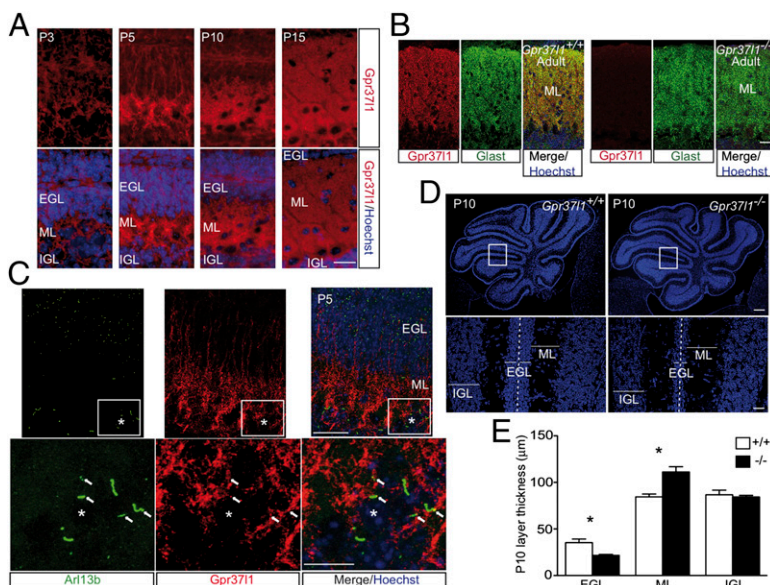

Fig. 1. *Gpr37l1* expression and cerebellar morphology of adult and developing *Gpr37l1*$^{+/+}$ and *Gpr37l1*$^{-/-}$ male mice. (A) Cerebellar immunofluorescence labeling of Gpr37l1 and nuclear Hoechst staining in P3, P5, P10, and P15 pups and (B) immunofluorescence labeling of Gpr37l1 (red) and Glast (green) in *Gpr37l1*$^{+/+}$ and *Gpr37l1*$^{-/-}$ adult mice. (C) Double immunofluorescence staining of Gpr37l1 and Arl13b in sagittal cerebellar sections of P5 wild-type pups. (D) Nuclear Hoechst staining in P10 cerebella of *Gpr37l1*$^{+/+}$ and *Gpr37l1*$^{-/-}$ pups. (E) Quantification of the average thickness of the EGL, ML, and IGL in the two genotype groups at P10 (mean ± SEM, n = 3 per group). *$P < 0.05$ $^{+/+}$ vs. $^{-/-}$, unpaired t test. (Scale bars in A–C, Upper, and D, Lower, 25 μm and in C, Lower, 10 μm and D, Upper, 250 μm.) EGL, external granular layer; IGL, internal granular layer; ML, molecular layer. Asterisks indicate Purkinje neuron somata; arrows point to Gpr37l1 and Arl13b doubly positive primary cilium structures.
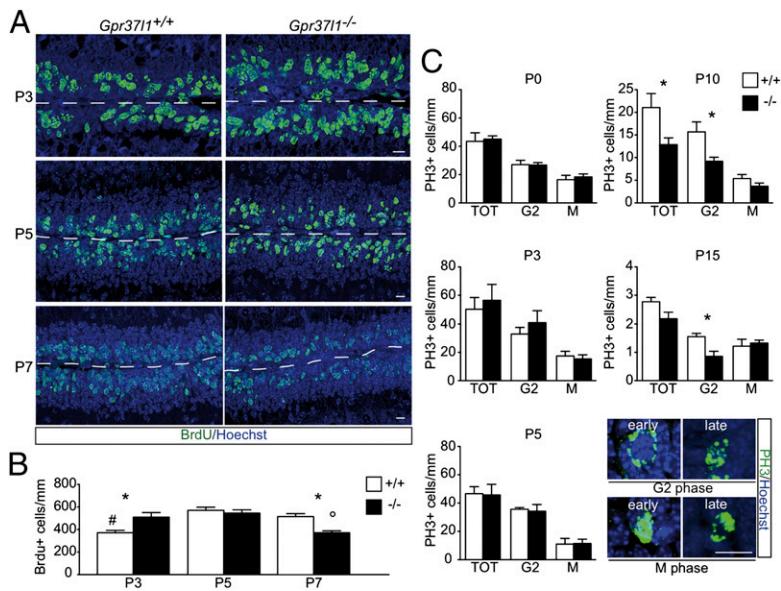
Fig. 2. Postnatal proliferation of cerebellar granule neuron precursors in $Gpr37l1^{+/+}$ and $Gpr37l1^{-/-}$ male mice. (*A*) Immunofluorescence labeling of BrdU and Hoechst staining of EGL cells at P3, P5, and P7 in $Gpr37l1^{+/+}$ and $Gpr37l1^{-/-}$ littermates. (*B*) Quantification of the average number of BrdU-positive cells normalized by the EGL length (mean ± SEM), *$P < 0.05$ +/+ vs. −/−; #$P < 0.05$ P3 vs. P5, P7 in $Gpr37l1^{+/+}$ mice; °$P < 0.05$ P7 vs. P3, P5 in $Gpr37l1^{-/-}$ mice, unpaired t test. (*C*) Quantification of the average number of phosphohistone H3 (PH3)-positive and G2- or M-phase cells at P0, P3, P5, P10, and P15 in the EGL of $Gpr37l1^{+/+}$ and $Gpr37l1^{-/-}$ littermates (mean ± SEM $n = 3$ per group), *$P \leq 0.05$ +/+ vs. −/−, unpaired t test. (*Lower*) Representative images of anti-PH3 immunofluorescence labeling and nuclear Hoechst counterstaining of EGL cells in P10 $Gpr37l1^{+/+}$ pups, showing distinct PH3-positive cells in either early or late G2 phase and either early or late (mitotic division) M phase. (Scale bars in *A* and *C*, 10 μm.)

that the proportion of Pcna-positive proliferating oEGL cells was similar in wild-type and $Gpr37l1^{-/-}$ littermates at P5, whereas it appeared increased at P3 and reduced at P10 in the mutant pups. The amount of Tag1-positive, differentiating iEGL cells appeared reduced at P3 and P10 in the $Gpr37l1^{-/-}$ animals and again very similar at P5 between the two genotypes (Fig. S3*A*). The two EGL cell subpopulations were quantitatively compared from P0 to P15, after total nuclear Hoechst staining combined with fluorescent anti–p27-Kip1 labeling. In the mutant pups, the total number of EGL-granule cells was significantly reduced at P10 and P15 [Fig. S3 *B and C*; ANOVA: effect of age, $F_{(4,28)} = 369.17$, $P < 0.0001$; effect of genotype, $F_{(1,28)} = 32.38$, $P < 0.0001$; age × genotype, $F_{(4,28)} = 11.9$, $P < 0.0001$], closely matching the genotype-dependent decrease in the overall EGL thickness at later developmental stages (Fig. 1*D* and Fig. S2). The number of Kip1-labeled iEGL neurons showed a significant decrement at P0, P10, and P15, whereas it was only marginally reduced at P3 and P5 [Fig. S3 *B and C*; ANOVA: effect of age, $F_{(4,28)} = 30.88$, $P < 0.0001$; effect of genotype, $F_{(1,28)} = 10.85$, $P = 0.0027$; age × genotype, $F_{(4,28)} = 1.18$, NS]. The number of oEGL, Kip1-negative cells appeared slightly increased at P3 and was significantly decreased at P10 [Fig. S3 *B and C*; ANOVA: effect of age, $F_{(4,28)} = 234.53$, $P < 0.0001$; effect of genotype, $F_{(1,28)} = 6.58$, $P = 0.016$; age × genotype, $F_{(4,28)} = 7.055$, $P = 0.0005$]. These results indicate a premature down-regulation of EGL proliferation with consequent reduction in the average EGL thickness (Figs. 1 and 2 and Figs. S2 and S3). These modifications were not associated with intrinsic alterations of the mechanisms of granule neuron migration to the IGL, as the proportion and distribution pattern of migrating cells were similar in wild-type and null mutant littermates (Fig. S4).

Precocious Bergmann Glia and Purkinje Neuron Maturation in $Gpr37l1^{-/-}$ Mice. Bergmann astrocytes were specifically stained with antibodies against nestin, glial fibrillary acidic protein (Gfap), brain lipid binding protein (Blbp), or Glast in sagittal cerebellar sections of $Gpr37l1^{-/-}$ and wild-type pups at various postnatal stages or adult animals (Figs. 1*B* and 3*A* and Fig. S5 *A–C*). Along with the reduction in EGL thickness, Glast immunostaining revealed the more expanded reticular domain of Bergmann fibers at P10 and P15 in $Gpr37l1^{-/-}$ pups (Fig. 3*A*) (23). No difference was detected with the other astrocytic markers (Fig. S5 *A–C*). The development of Purkinje neurons was analyzed by specific immunolabeling of calbindin 1 (or calbindin D-28K; Calb1) in sagittal cerebellar sections of $Gpr37l1^{-/-}$ and wild-type pups at P5, P10, P15, and P20 (Fig. 3*B* and Fig. S5 *D and E*). The $Gpr37l1^{-/-}$ animals showed

earlier alterations in the cell body alignment and dendritic arborization at P10 and P15 in comparison with their wild-type littermates. Qualitative analysis revealed a more extended and elaborate architecture of the dendritic trees and a better alignment of cell bodies (Fig. 3*B*), indicating a precocious maturation of the Purkinje neurons (24). The measurement of the average intensity and discrete extension of Calb1 immunolabeling confirmed that Purkinje arborizations that form the cerebellar ML
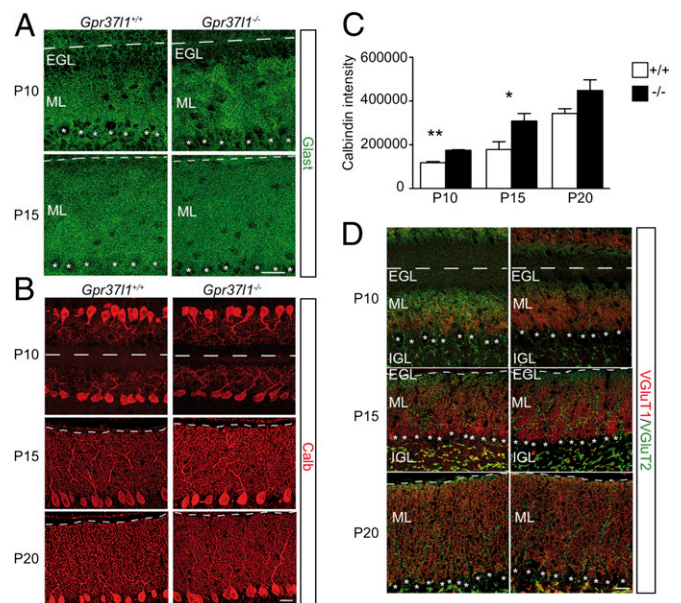

Fig. 3. Postnatal maturation of Bergmann glia and Purkinje neurons in $Gpr37l1^{+/+}$ and $Gpr37l1^{-/-}$ male mice. (*A*) Immunofluorescence labeling of Glast in P10 and P15 cerebella of $Gpr37l1^{+/+}$ and $Gpr37l1^{-/-}$ littermates. (*B*) Immunofluorescence labeling of Calb in P10, P15, and P20 cerebella of $Gpr37l1^{+/+}$ and $Gpr37l1^{-/-}$ littermates. (*C*) Quantification of Calb immunostaining intensity. Data are expressed in arbitrary units (mean ± SEM, $n = 3$ per group), *$P = 0.057$, **$P < 0.001$ +/+ vs. −/−, unpaired t test. (*D*) Double immunofluorescence staining of VGluT1 and VGluT2 in P10, P15, and P20 cerebella of $Gpr37l1^{+/+}$ and $Gpr37l1^{-/-}$ littermates. (Scale bars in *A*, *B*, and *D*, 25 μm.) EGL, external granular layer; IGL, internal granular layer; ML, molecular layer. Asterisks indicate Purkinje neuron somata.

were significantly more developed at P10 and P15 in $Gpr37l1^{-/-}$ pups [Fig. 4C; ANOVA: effect of age, $F_{(2,12)} = 35.85$, $P < 0.0001$; effect of genotype, $F_{(1,12)} = 16.05$, $P = 0.0017$; age × genotype, $F_{(2,12)} = 0.77$, NS]. These data are in agreement with the measured increase in the average ML thickness at P10 in the null mutant pups (Fig. 1 *D* and *E*). Specific double immunolabeling of vesicular glutamate transporter 1 (Vglut1) and vesicular glutamate transporter 2 (Vglut2) was used to analyze the development from P10 to P20 of axonal afferents of granule cell parallel fibers (PFs) or inferior olivary nucleus climbing fibers (CFs) to Purkinje cell distal arbor or proximal stem dendrites, respectively (Fig. 3*D* and Fig. S5*F*) (25, 26). At P10 and P15 the $Gpr37l1^{-/-}$ pups showed a prevalence of Vglut1-positive, granule cell PFs, indicating an increased extension in their synaptic terminals onto the more developed distal branchlets of Purkinje dendrites (Fig. 3 *B* and *D*). At P10 the perisomatic to peridendritic translocation of Vglut2-positive CFs was also more advanced in P10 $Gpr37l1^{-/-}$ pups. At P15, CF terminals extended for most of the ML thickness, whereas in the control pups, they were confined to the deep ML region. No difference was evident at P20, when Purkinje arborization did not significantly vary between $Gpr37l1^{-/-}$ and wild-type littermates (Fig. 3 *B* and *D*).

Early Activation of the Shh-Mediated Mitogenic Pathway in $Gpr37l1^{-/-}$ Cerebella. The above results suggest the altered regulation in $Gpr37l1^{-/-}$ pups of cerebellar neuron proliferation and post-mitotic differentiation mechanisms that are known to be under the control of the mitogenic Shh–Ptch1–Smo signaling pathway (7–9). Therefore, the expression levels of several protein components of the Shh signaling cascade were compared by immunoblot analysis of cerebellar tissue extracts of $Gpr37l1^{-/-}$ and wild-type littermates, at various postnatal stages (Fig. 4*A*). The average level of Purkinje-cell–secreted Shh mitogen was markedly increased at P5 in $Gpr37l1^{-/-}$ samples [ANOVA: effect of genotype, $F_{(1,12)} = 6.62$, $P < 0.05$]. Wild-types showed a tendency to a later (P10) increase in the Shh levels compared with P5, whereas both genotype groups had a comparable decrease at P15, as reported (27). In null mutant extracts the level of Shh coreceptor Smo was increased at P5 and decreased at P10 and P15, whereas wild-type controls showed an increment only at later postnatal stages [ANOVA: effect of age, $F_{(2,12)} = 14.49$, $P = 0.0006$; effect of genotype, $F_{(1,12)} = 4.80$, $P < 0.05$; age × genotype, $F_{(2,12)} = 25.97$, $P < 0.0001$]. Consistently, the levels of the Shh receptor inhibitory component Ptch1, were significantly higher at P5 and P10 in the $Gpr37l1^{-/-}$ extracts. The levels of the intracellular effectors of the Shh-Smo cascade, neuroblastoma-derived myelocytomatosis viral-related oncogene (*N*-Myc),

glioma-associated oncogene family zinc finger 2 (Gli2), and eukaryotic initiation factor 4E (eIF4), were also assayed at P5 and decreased at P10 in $Gpr37l1^{-/-}$ pups in comparison with wild-type controls [ANOVA, age × genotype effects: *N*-Myc, $F_{(2,12)} = 21.73$, $P = 0.0001$; Gli2, $F_{(2,12)} = 11.43$, $P = 0.0017$; EIF4, $F_{(2,12)} = 15.00$, $P = 0.0005$].

Gpr37l1 Colocalizes and Interacts with Ptch1 in Bergmann Glia Cells. Coimmunolabeling on sagittal cerebellar sections from P3 and P10 wild-type pups revealed a colocalization of the Gpr37l1 and Ptch1 proteins in Bergmann astrocyte membranes (Fig. 4*B*). Gpr37l1 and Ptch1 interaction was assayed by specific coimmunoprecipitation in $Gpr37l1^{-/-}$ and wild-type lysates of P10 cerebella. Anti-Ptch1 incubation and immunoblotting with anti-Gpr37l1 showed that the receptor was specifically coprecipitated in wild-type samples only (Fig. 4*C*). The Gpr37l1 antibody specifically coprecipitated the Ptch1 protein in wild-type but not in $Gpr37l1^{-/-}$ lysates (Fig. 4*D*). Control experiments showed that Ptch1 was precipitated by its specific antibody, in both $Gpr37l1^{-/-}$ and wild-type samples, whereas anti-Gpr37l1 induced specific precipitation in wild-type lysates only (Fig. 4 *C* and *D*). No specific coimmunoprecipitation of the Gpr37l1 and Smo proteins was detected in wild-type or $Gpr37l1^{-/-}$ lysates (Fig. S5*G*).

$Gpr37l1^{-/-}$ Mice Show Improved Motor Learning. Alterations of postnatal cerebellar layering and Purkinje neuron maturation can be associated with permanent changes of motor and learning functions. $Gpr37l1^{-/-}$ and wild-type littermates were subjected to behavioral analysis at various ages, from early development to weaning and adulthood. No differences between genotypes were found in body measures, physical landmarks, or other sensory reflexes in 2- to 20-d-old male and female pups (Fig. S6). The only exception was precocious eye opening observed in $Gpr37l1^{-/-}$ male pups (Fig. S6*B*). From the initial stages of sensorimotor development, $Gpr37l1^{-/-}$ male mice showed a stronger negative geotaxis reflex than wild types (i.e., shorter latency to rotate head up when placed facing down on an inclined plane) [Fig. 5*A*, repeated-measures (RM) ANOVA, genotype effect, $F_{(2,19)} = 3.99$, $P < 0.05$], and higher scores for climbing reflex at P10 (Fig. 5*B*). Also, duration of bar holding at P10 [Fig. 5*C*, ANOVA, genotype effect, $F_{(2,25)} = 3.35$, $P = 0.05$] and wire hanging at P20 tended to be longer in the mutants (Fig. 5*C*), pointing to better motor performance.

Motor coordination performance was then assessed in a different cohort of adult $Gpr37l1^{-/-}$ male mice at different ages. Mutants showed shorter latencies to turn in the pole test, more markedly at 7 mo [Fig. 5*D*, *Upper*, RM ANOVA, genotype effect,
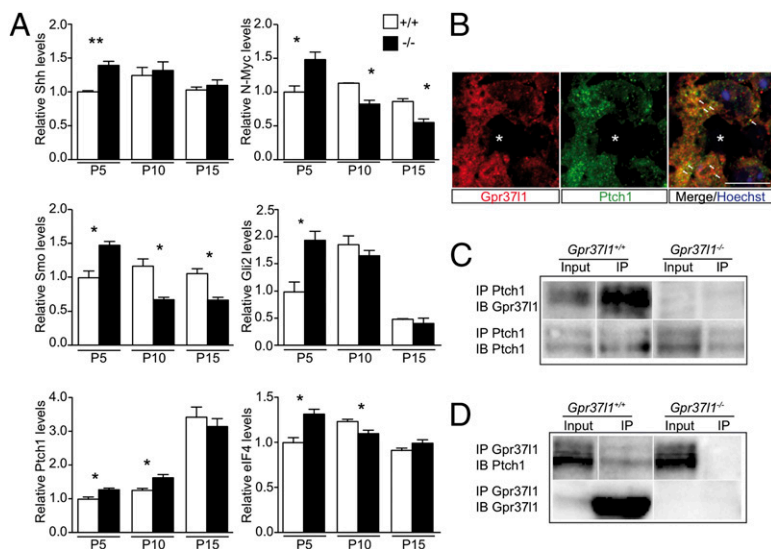

Fig. 4. Postnatal cerebellar Shh signaling and Gpr37l1–Ptch1 interaction in $Gpr37l1^{+/+}$ and $Gpr37l1^{-/-}$ male mice. (*A*) Immunoblotting and densitometric quantification of Shh pathway proteins in whole cerebellar extracts prepared at P5, P10, and P15 from $Gpr37l1^{+/+}$ and $Gpr37l1^{-/-}$ littermate pups (mean ± SEM, $n = 3$ mice per group), *$P < 0.05$, **$P < 0.005$ $^{+/+}$ vs. $^{-/-}$, unpaired *t* test. (*B*) Double immunofluorescence staining of Gpr37l1 and Ptch1 in sagittal cerebellar sections of P3 wild-type pups. (*C* and *D*) Coimmunoprecipitation analysis of Ptch1 and Gpr37l1 in cerebellar extracts from P10 $Gpr37l1^{+/+}$ and $Gpr37l1^{-/-}$ littermates. Immunoprecipitations (IP) were performed with the Ptch1 or Gpr37l1 antibody followed by immunoblotting for the indicated proteins. A representative result from three distinct experiments is shown. (Scale bars, 10 μm.) Asterisks indicate Purkinje neuron somata; arrows point to doubly positive Bergmann glia cells.
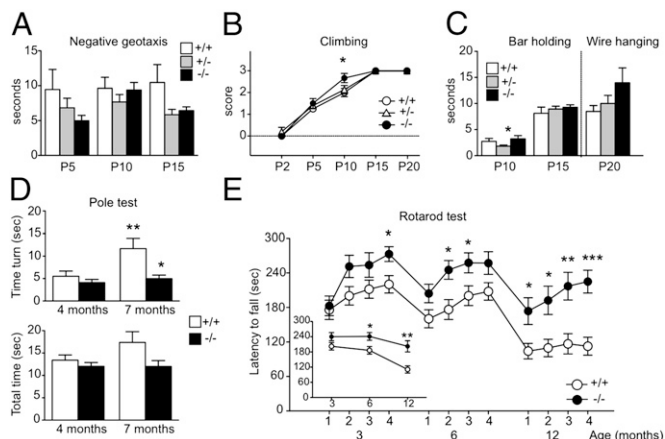
Fig. 5. Behavioral analysis of newborn and adult $Gpr37l1^{+/+}$ and $Gpr37l1^{-/-}$ littermates. (A–C) Negative geotaxis latency, climbing score, bar holding, and wire hanging time measured in male mice at P2, P5, P10, P15, and P20. *$P <$ 0.05 $^{+/+}$ vs. $^{-/-}$ or $^{+/-}$ vs. $^{-/-}$, unpaired t test. $^{+/+}$ $n = 7–8$; $^{+/-}$ $n = 13–15$; $^{-/-}$ $n = 5–6$. (D) Pole test performed in adult male mice at 4 and 7 mo. Bars represent the time to turn downward (*Upper* graph) and the total time to climb down (*Lower* graph). *$P < 0.05$, $^{+/+}$ vs. $^{-/-}$, **$P < 0.005$, 4 vs. 7 mo in $^{+/+}$ group, unpaired t test. $^{+/+}$ $n = 16$; $^{-/-}$ $n = 13$. (E) Rotarod test performed in adult male mice at 3, 6, and 12 mo; open ($^{+/+}$) and solid ($^{-/-}$) circles represent the latency to fall off the rod over 4 d (mean of three trials per day); in the *Inset* the latency to fall at 3, 6, and 12 mo, averaged across 4 d per age group (mean ± SEM). *$P <$ 0.05; **$P < 0.005$; ***$P < 0.0001$, $^{+/+}$ vs. $^{-/-}$ unpaired t test. $^{+/+}$ $n = 17$; $^{-/-}$ $n = 12$.

$F_{(1,27)} = 5.02, P < 0.05$; age × genotype effect, $F_{(1,27)} = 5.72, P < 0.05$], and a tendency to climb down faster than wild-type littermates, (Fig. 5D, *Lower*). Significantly improved motor coordination performance and motor learning were finally observed in adult $Gpr37l1^{-/-}$ male mice compared with wild-type littermates (Fig. 5E). Especially at 6 and 12 mo, mutant mice showed longer latencies to fall from the accelerating rotarod over 4 d of testing [Fig. 5E, RM ANOVA, genotype effect, $F_{(1,27)} = 8.958, P = 0.0058$; age × genotype effect, $F_{(2,54)} = 4.57$, $P < 0.05$; day × genotype effect, $F_{(3,81)} = 3.55, P < 0.05$].

Discussion

This study shows that the Gpr37l1 receptor is expressed in Bergmann glia astrocytes of newborn and adult mice. During postnatal cerebellar development, it participates in the regulation of granule neuron proliferation/differentiation, Bergmann glia and Purkinje neuron maturation, and Shh mitogenic signaling. Furthermore, it interacts with the Ptch1 transporter-like component of the Shh receptor complex. The reported immunolabeling analysis reveals that the Gpr37l1 protein is specifically and progressively expressed in cell bodies and fibrous processes of cerebellar Bergmann glia from the earliest neonatal phases to the adult stage (Fig. 1 A and B), whereas it is not expressed in newborn and adult cerebellar granule and Purkinje neuronal cells, as reported (15, 17, 28). Thus, Gpr37l1 is a specific marker of murine Bergmann astrocytes. Its expression pattern closely matches Glast immunostaining in glial fibers (23), since the earliest postnatal stages (Fig. 1 A and B). These fibers establish specific glial-neuronal intercellular interactions and regulate migration and differentiation of postmitotic granule and the maturation of Purkinje neurons (2, 3), suggesting the involvement of Gpr37l1 in the regulation of postnatal cerebellar development. Genetic ablation of Gpr37l1 results in the premature down-regulation of proliferation and altered postmitotic differentiation of EGL precursors and maturation of Bergmann fibers that parallels the early layering of Purkinje neurons and differentiation of their dendritic arborization and afferent synaptic wiring (Figs. 2 and 3 and Figs. S2–S5). These phenotypic modifications occur and progress within a limited time frame in null mutant newborns, as no cytohistological and anatomical

differences between $Gpr37l1^{-/-}$ and wild-type cerebella were detected from approximately P20 onwards (Fig. 3 and Figs. S2 and S5).

Several other gene knock-out models show altered proliferation and differentiation of the EGL precursors, but, contrary to the $Gpr37l1^{-/-}$ strain, they also present uncontrolled or malignant expansion of the granule neurons and/or disruption of their migratory process to IGL (29, 30). Moreover, most reported mutant phenotypes that affect Purkinje neurons are associated with cytological, biochemical changes that last up to the postweaning or adult age (31, 32). Thus, the Gpr37l1 null mutant line can be a model for structural cerebellar changes that are temporally restricted to the early postnatal stages and result in specific phenotypes of motor function development and related behaviors.

The improved motor functions of adult $Gpr37l1^{-/-}$ males may be linked to their early cerebellar development, with precocious layering and maturation of Purkinje neurons. This would be consistent with differences in motor abilities and eye opening observed in mutant pups (Fig. 5 and Fig. S6). Improved motor learning has been described in mice lacking the Purkinje cell protein 2/L7 (33), a G-protein modulator. Gene knock-out strains of Glast (34), vimentin (35), and neuronal cell adhesion protein (36) exhibit various defects in Bergmann glia cells but no enhancement of motor functions.

Right after birth, Purkinje cells secrete cholesterol-modified Shh protein, which stimulates GCP proliferation (7–9) and promotes Bergmann glia's postnatal maturation (7). Stimulated cerebellar astrocytes and GCPs express the seven-membrane span, Shh effector Smo, and membrane transporter-like, Shh-Smo corepressor Ptch1 (10, 11). Concomitant with the premature down-regulation of GCP proliferation, $Gpr37l1^{-/-}$ pups showed an early cerebellar overexpression of the Shh mitogen, its effector Smo, and transcription activators such as N-Myc and Gli2. The overexpression of Shh is also associated with an early increase in the levels of the Smo corepressor Ptch1 (Fig. 4). This would promote early feedback signals that cause premature cell cycle exit of GCPs and induce their postmitotic migration and maturation (37). However, some caution should be taken when analyzing whole cerebellar extracts as these also contain non-GCP fractions. Combined in vitro primary cell culture and fractionation systems could be used for a comparative investigation of Shh and related signaling components in the various cerebellar glial and neuronal cell types.

Gpr37l1 is known to be widely expressed in adult cerebellar Bergmann astrocytes but this study demonstrates that it is specifically coexpressed, and interact and colocalize with the Ptch1 protein in discrete areas of Bergmann glia cell membranes in newborn mice (Fig. 4). Ptch1 and associated components of the Shh-Smo mitogenic pathway are organized in specialized primary cilia of pre- and postnatal cerebellar astrocytes and neurons (11, 38). Gpr37l1 has been identified as a modulator of neuronal primary ciliogenesis (18). It also colocalizes with Arl13b in Bergmann glia cilia (Fig. 1C), where it may be involved in regulating Shh-Smo ciliary signaling. The Gpr37 protein, a paralog of Gpr37l1 (39) interacts with and modulates the dopamine transporter that is structurally similar to Ptch1. The mammalian Gpr37-like, putative G-protein–coupled receptors could therefore exert specific regulatory roles by interacting with membrane transporter-like proteins.

Shh signaling has been reported to induce and modulate the differentiation/maturation of cerebellar astrocytes (7). Glast immunolabeling (23, 40) (Fig. 3) shows that $Gpr37l1^{-/-}$ pups have expanded Bergmann fiber reticules, along with reduced EGL thickness and enhanced Purkinje dendrite's arborization and connectivity. Conceivably, Gpr37l1 may be important in the activation of developing cerebellar glia, via still unknown ligands, whose production is temporally limited to the peri- and postnatal stages. Recently, the secreted neuro- and glioprotective glycoprotein prosaposin and derived peptides have been shown in vitro to activate the putative Gpr37l1 and Gpr37 receptors (22).

Prosaposin and other secreted proteins are produced by Purkinje neurons of newborn mice, with very low expression in prenatal and adult stages (41–45). They could specifically activate postnatal Gpr37l1 signaling in Bergmann astrocytes. Gpr37l1 has been identified as a modulator of primary ciliogenesis (18), and this study reports its membrane association with the Shh coreceptor Ptch1 (Fig. 4). Thus, Gpr37l1 ablation may alter the Ptch1-controlled astrocytic ciliary assembly and functional interactions with Purkinje neurons and GCPs at the earliest postnatal stages. Such alterations could lead to increased Shh secretion by Purkinje neurons, followed by activation of the Ptch1-mediated inhibition of Smo signaling in GCPs. This would, in turn, result in the observed early termination of granule neuron proliferation, reduction in EGL thickness, and expansion of astrocytic reticular fibers, with consequent precocious layering and dendritic maturation of Purkinje neurons.

Materials and Methods

Detailed materials and methods are given in *SI Materials and Methods*.

Immunofluorescence. Age-matched brains from male null mutant mice and their wild-type littermates were dissected, fixed in 4% wt/vol paraformaldehyde, dehydrated, and embedded in paraffin for microtome serial sectioning (8-μm thickness). Specific primary and secondary antibodies were used as described in *SI Materials and Methods*.

Western Blot Analysis. Protein extracts were prepared from the cerebella of $Gpr37l1^{-/-}$ or wild-type male pups at different postnatal developmental stages (P5, P10, and P15). Specific antibodies were used as described in *SI Materials and Methods*.

Immunoprecipitation. Cerebella from P10 $Gpr37l1^{-/-}$ or wild-type male pups were solubilized and processed with specific antibodies as described in *SI Materials and Methods*.

Behavioral Tests. Motor coordination and learning were tested in adult male mice at various ages from 3 to 12 mo, and postnatal milestones were tested from P2 to P20 as described in *SI Materials and Methods*.

1. Sotelo C (2004) Cellular and genetic regulation of the development of the cerebellar system. *Prog Neurobiol* 72(5):295–339.
2. Gao WO, Heintz N, Hatten ME (1991) Cerebellar granule cell neurogenesis is regulated by cell-cell interactions in vitro. *Neuron* 6(5):705–715.
3. Rakic P (1971) Neuron-glia relationship during granule cell migration in developing cerebellar cortex. A Golgi and electronmicroscopic study in Macacus Rhesus. *J Comp Neurol* 141(3):283–312.
4. Yue Q, et al. (2005) PTEN deletion in Bergmann glia leads to premature differentiation and affects laminar organization. *Development* 132(14):3281–3291.
5. Tanaka S, Shaikh IM, Chiocca EA, Saeki Y (2009) The Gs-linked receptor GPR3 inhibits the proliferation of cerebellar granule cells during postnatal development. *PLoS ONE* 4(6):e5922.
6. Roussel MF, Hatten ME (2011) Cerebellum development and medulloblastoma. *Curr Top Dev Biol* 94:235–282.
7. Dahmane N, Ruiz i Altaba A (1999) Sonic hedgehog regulates the growth and patterning of the cerebellum. *Development* 126(14):3089–3100.
8. Wallace VA (1999) Purkinje-cell-derived Sonic hedgehog regulates granule neuron precursor cell proliferation in the developing mouse cerebellum. *Curr Biol* 9(8):445–448.
9. Wechsler-Reya RJ, Scott MP (1999) Control of neuronal precursor proliferation in the cerebellum by Sonic Hedgehog. *Neuron* 22(1):103–114.
10. Vaillant C, Monard D (2009) SHH pathway and cerebellar development. *Cerebellum* 8(3):291–301.
11. Ruat M, Roudaut H, Ferent J, Traiffort E (2012) Hedgehog trafficking, cilia and brain functions. *Differentiation* 83(2):S97–S104.
12. Izzi L, et al. (2011) Boc and Gas1 each form distinct Shh receptor complexes with Ptch1 and are required for Shh-mediated cell proliferation. *Dev Cell* 20(6):788–801.
13. Allen BL, et al. (2011) Overlapping roles and collective requirement for the coreceptors GAS1, CDO, and BOC in SHH pathway function. *Dev Cell* 20(6):775–787.
14. Ho KS, Scott MP (2002) Sonic hedgehog in the nervous system: Functions, modifications and mechanisms. *Curr Opin Neurobiol* 12(1):57–63.
15. Sato A, et al. (2008) Cerebellar development transcriptome database (CDT-DB): Profiling of spatio-temporal gene expression during the postnatal development of mouse cerebellum. *Neural Netw* 21(8):1056–1069.
16. Lein ES, et al. (2007) Genome-wide atlas of gene expression in the adult mouse brain. *Nature* 445(7124):168–176.
17. Valdenaire O, et al. (1998) A new family of orphan G protein-coupled receptors predominantly expressed in the brain. *FEBS Lett* 424(3):193–196.
18. Kim J, et al. (2010) Functional genomic screen for modulators of ciliogenesis and cilium length. *Nature* 464(7291):1048–1051.
19. Huangfu D, et al. (2003) Hedgehog signalling in the mouse requires intraflagellar transport proteins. *Nature* 426(6962):83–87.
20. Marazziti D, et al. (1997) Cloning of GPR37, a gene located on chromosome 7 encoding a putative G-protein-coupled peptide receptor, from a human frontal brain EST library. *Genomics* 45(1):68–77.
21. Marazziti D, Gallo A, Golini E, Matteoni R, Tocchini-Valentini GP (1998) Molecular cloning and chromosomal localization of the mouse Gpr37 gene encoding an orphan G-protein-coupled peptide receptor expressed in brain and testis. *Genomics* 53(3):315–324.
22. Meyer RC, Giddens MM, Schaefer SA, Hall RA (2013) GPR37 and GPR37L1 are receptors for the neuroprotective and glioprotective factors prosaptide and prosaposin. *Proc Natl Acad Sci USA* 110(23):9529–9534.
23. Yamada K, et al. (2000) Dynamic transformation of Bergmann glial fibers proceeds in correlation with dendritic outgrowth and synapse formation of cerebellar Purkinje cells. *J Comp Neurol* 418(1):106–120.
24. Hatten ME, Heintz N (1995) Mechanisms of neural patterning and specification in the developing cerebellum. *Annu Rev Neurosci* 18:385–408.
25. Fremeau RT, Jr., et al. (2001) The expression of vesicular glutamate transporters defines two classes of excitatory synapse. *Neuron* 31(2):247–260.
26. Miyazaki T, Fukaya M, Shimizu H, Watanabe M (2003) Subtype switching of vesicular glutamate transporters at parallel fibre-Purkinje cell synapses in developing mouse cerebellum. *Eur J Neurosci* 17(12):2563–2572.
27. Corrales JD, Rocco GL, Blaess S, Guo Q, Joyner AL (2004) Spatial pattern of sonic hedgehog signaling through Gli genes during cerebellum development. *Development* 131(22):5581–5590.
28. Leng N, Gu G, Simerly RB, Spindel ER (1999) Molecular cloning and characterization of two putative G protein-coupled receptors which are highly expressed in the central nervous system. *Brain Res Mol Brain Res* 69(1):73–83.
29. Hatten ME, Roussel MF (2011) Development and cancer of the cerebellum. *Trends Neurosci* 34(3):134–142.
30. Behesti H, Marino S (2009) Cerebellar granule cells: Insights into proliferation, differentiation, and role in medulloblastoma pathogenesis. *Int J Biochem Cell Biol* 41(3):435–445.
31. Dusart I, Flamant F (2012) Profound morphological and functional changes of rodent Purkinje cells between the first and the second postnatal weeks: A metamorphosis? *Front Neuroanat* 6:11.
32. Sotelo C, Dusart I (2009) Intrinsic versus extrinsic determinants during the development of Purkinje cell dendrites. *Neuroscience* 162(3):589–600.
33. Iscru E, et al. (2009) Sensorimotor enhancement in mouse mutants lacking the Purkinje cell-specific Gi/o modulator, Pcp2(L7). *Mol Cell Neurosci* 40(1):62–75.
34. Watase K, et al. (1998) Motor discoordination and increased susceptibility to cerebellar injury in GLAST mutant mice. *Eur J Neurosci* 10(3):976–988.
35. Colucci-Guyon E, Giménez Y Ribotta M, Maurice T, Babinet C, Privat A (1999) Cerebellar defect and impaired motor coordination in mice lacking vimentin. *Glia* 25(1):33–43.
36. Yang W, Li C, Mansour SL (2001) Impaired motor coordination in mice that lack punc. *Mol Cell Biol* 21(17):6031–6043.
37. Rohatgi R, Milenkovic L, Scott MP (2007) Patched1 regulates hedgehog signaling at the primary cilium. *Science* 317(5836):372–376.
38. Chizhikov VV, et al. (2007) Cilia proteins control cerebellar morphogenesis by promoting expansion of the granule progenitor pool. *J Neurosci* 27(36):9780–9789.
39. Marazziti D, et al. (2007) GPR37 associates with the dopamine transporter to modulate dopamine uptake and behavioral responses to dopaminergic drugs. *Proc Natl Acad Sci USA* 104(23):9846–9851.
40. Shibata T, et al. (1997) Glutamate transporter GLAST is expressed in the radial glia-astrocyte lineage of developing mouse spinal cord. *J Neurosci* 17(23):9212–9219.
41. Kreda SM, Fujita N, Suzuki K (1994) Expression of sphingolipid activator protein gene in brain and systemic organs of developing mice. *Dev Neurosci* 16(1–2):90–99.
42. Sun Y, Witte DP, Grabowski GA (1994) Developmental and tissue-specific expression of prosaposin mRNA in murine tissues. *Am J Pathol* 145(6):1390–1398.
43. Müller T, Kettenmann H (1995) Physiology of Bergmann glial cells. *Int Rev Neurobiol* 38:341–359.
44. Basille-Dugay M, et al. (2013) Spatio-temporal characterization of the pleiotrophinergic system in mouse cerebellum: Evidence for its key role during ontogenesis. *Exp Neurol* 247:537–551.
45. Xue B, et al. (2011) Chronological changes in prosaposin in the developing rat brain. *Neurosci Res* 71(1):22–34.

DEVELOPMENTAL BIOLOGY